J. Electroanal. Chem., 310 (1991) 361–377
Elsevier Sequoia S.A., Lausanne

Changes in the growth mode of electrodeposited silver layers

Surface rearrangements induced by the presence of lead adatoms

P. Carro, A. Hernández Creus, S. González, R.C. Salvarezza [1] and A.J. Arvia [1]

Departamento de Química Física, Universidad de La Laguna, 38201 La Laguna, Tenerife (Spain)

(Received 28 August 1990; in revised form 11 January 1991)

Abstract

The surface characteristics of Ag electrodeposits prepared on polyfaceted Pt(sc) electrodes have been followed through complete Pb upd/stripping voltammetry. The growth mode of Ag overlayers at constant temperature depends on both the cathodic electrodeposition overvoltage and the silver ion concentration in solution. Ag surface rearrangements can be induced by either holding the potential or Pb upd/stripping cycling in the potential range where the degree of surface coverage by Pb adatoms is between 0 and 1. The voltammograms of Ag overlayers at the monolayer level show considerable changes compared with those obtained for thicker Ag overlayers. The present results allow us to establish a correlation between the development of rough electrodeposits and the surface diffusion properties of metal atoms.

(I) INTRODUCTION

In electrochemistry, particularly metal electrocrystallization, extensive studies have been carried out on the topography of electrode metal deposits and its dependence on the preparation conditions [1]. It was shown, for instance, that the growth mode of these electrodeposits becomes extremely dependent on the electroreduction potential conditions [2–4], the solution composition [5] and the temperature [6]. By changing these variables in the proper way, different types of rough surfaces, crystallographic orientations, and, correspondingly, catalytic properties of the metal overlayers can be obtained [7–9]. The main aim of the present work was the determination of the electrochemical characteristics of Ag overlayers of different

[1] Visiting Professor from INIFTA, Facultad de Ciencias Exactas, Universidad de La Plata, La Plata, Argentina.

0022-0728/91/$03.50

average thicknesses formed on foreign substrates under different electrodeposition conditions. For this purpose, the complete Pb upd/stripping voltammogram was used as reference. These reactions have been investigated recently in several laboratories [10–15], oriented principally to determine the Pb upd behaviour on Ag single crystals under different potential routines. However, as the Pb upd/stripping cycling can induce surface rearrangements of Ag overlayers, a fact which can invalidate the use of this reversible electrochemical system to follow the characteristics of Ag overlayers, as part of the present work the conditions for minimum and maximum Ag overlayer restructuring induced by Pb upd/stripping cycling were also established in order to determine the possible use of the complete Pb upd/stripping reactions as test reactions for the main purpose of the work.

Despite the gap existing between the surface science of metal/low pressure gas phase and metal/electrolyte solution systems [16], the effects described in the present work appear to be qualitatively comparable to those described for both the growth mode of metal overlayers and the adsorption/desorption-induced metal surface restructuring in metal/gas phase systems [17–19].

(II) EXPERIMENTAL

Preliminary experiments were performed on different substrate electrodes, such as Ag microspheres and Ag wires with and without annealing, Pt polycrystalline (pc) plate, Pt (pc) preferred oriented, and polyfaceted Pt single crystal (sc) microspheres, in order to select the best working electrode substrate for the present study. Accordingly, most of the work was carried out principally on polyfaceted Pt (sc) microsphere working electrodes of ca. 0.03 cm^2 geometric area. These electrodes were prepared from Pt (pc) wires by the usual melting technique [20]. A large Pt plate and a saturated calomel electrode (SCE) were used as the counter-electrode and reference electrode, respectively. Potentials in the text are referred to the SCE scale. The three electrodes were mounted in a conventional Pyrex glass electrochemical cell.

The following electrolyte solutions were employed: (i) 0.5 M $NaClO_4$ + 10^{-2} M $HClO_4$ (solution A); (ii) x M Ag_2SO_4 + 0.5 M $NaClO_4$ + 10^{-2} M $HClO_4$ ($5 \times 10^{-5} < x < 5 \times 10^{-3}$) (solution B); and (iii) 10^{-2}M Pb(acetate)$_2$ + 0.5 M $NaClO_4$ + 10^{-2} M $HClO_4$ (solution C). Solutions were prepared from MilliQ* water and A.R. chemicals. Water purity was tested by repetitive potential cycling of a Pt electrode in 0.5 M H_2SO_4 in the H-electrosorption potential range [21]. Before each run, solutions were deaerated by bubbling purified Ar for 30 min. Special care was taken to eliminate not only O_2 from the system, as it distorted the Pb upd/stripping voltammograms, but also any other type of traceable impurity. Extremely clean laboratory conditions, and gas ducts and protective traps made entirely of glass were required to achieve reproducible and reliable results.

The electrochemical runs consisted in the following stages: (i) The voltammetric characterization of the substrate surface in solution A. (ii) The Ag electrodeposition on the substrate surface done at a constant potential, E_d, in solution B. The value of

E_d was changed in the 0 V < E_d < E_r range, E_r being the reversible potential of the Ag/Ag^+ ion electrode. (iii) Pb upd/stripping cycling was run in solution C at 0.01 V/s between 0 V and $E_r(Pb/Pb^{2+}) = -0.427$ V (vs. SCE). The different operations involve transfer of the working electrode from solution B to solution C. Blank experiments showed that under the carefully controlled conditions of the present experiments no artifacts assigned to these operations could be detected. Runs were made at 25 °C.

The Ag overlayer characteristics as well as the changes induced by several potential routines were followed through the complete Pb upd/stripping voltammograms run at 0.01 V/s between 0 and −0.420 V (conventional Pb upd/stripping voltammetry). The voltammetric data reported in the literature for well-defined Ag single-crystal surfaces were taken as reference [10–15]. Conventional Pb upd/stripping voltammograms implied negligible Ag restructuring, i.e. the shape of the conventional Pb stripping voltammogram remained very close to that of the first positive potential-going scan, except for a small decrease in the voltammetric charge during cycling, as described later.

(III) RESULTS

(III.1) The choice of the substrate electrode

For the present study the influence of the metal substrate on the electrochemical characteristics of Ag overlayers is important, particularly as the thickness of the thin Ag overlayer approaches the monolayer (ML) thickness. The most suitable substrate was selected by looking at the shape and the reproducibility of conventional Pb upd/stripping voltammograms obtained for Ag overlayers of different thicknesses on the various substrates. It was found that for very thin Ag overlayers the voltammograms became sensitive to the preparation conditions of the Ag overlayers, but for constant Ag overlayer average thickness and preparation conditions, the best voltammetric reproducibility was obtained on polyfaceted Pt (sc) electrodes. Therefore, the results obtained with this type of electrode are presented in the following sections.

(III.2) Electrochemically induced rearrangements at Ag electrodeposits

Pb upd/stripping cycling involving switching potential values and sweep rate conditions for which only a fractional value of θ_{Pb}, the degree of surface coverage by Pb adatoms, produces remarkable changes in the conventional Pb upd/stripping voltammogram run afterwards. To determine whether the dynamics of the Ag surface are either intrinsically coupled to the proper Pb upd/stripping processes or are simply due to the presence of Pb atoms at the Ag surface, runs were made in two directions; namely, to attempt to induce Ag surface rearrangements either at a constant potential or under potential cycling in the Pb upd/stripping potential

range by choosing different lower switching potentials, so that in both cases fractional values of θ_{Pb} were involved in the process.

(III.2.1) The influence of potential holding in the $0 < \theta_{Pb} < 1$ potential range

When a Ag overlayer which exhibits the Pb upd/stripping voltammogram depicted in Fig. 1a is held for 10 min at $E = -0.285$ V, i.e. at a potential value where $\theta_{Pb} = 0.6$, the subsequent conventional Pb upd/stripping voltammogram (Fig. 1b) changes drastically compared with the initial one. Thus, the new voltammogram (Fig. 1b), which exhibits a rather broad reversible Pb upd/stripping pair of peaks at -0.275 V together with a relatively extended complex irreversible Pb stripping peak covering the -0.175 to -0.125 V range, suggests a considerable increase in disorder at the Ag surface. Furthermore, the new irreversible Pb stripping peak indicates that a fraction of the Pb adatoms have presumably moved into bulk Ag to form a Pb + Ag alloy. Alloying effects in metal upd have already been reported for other systems [22,23]. At this stage, the subsequent conventional voltammogram (Fig. 1c) still exhibits a complex structure, although with a tendency to return to the initial voltammogram (Fig. 1a). Finally, continuous potential cycling under conventional conditions leads to the voltammogram depicted in Fig. 1d, which is practically coincident with the initial one. Therefore, conventional potential cycling between 0 and -0.420 V, in contrast to the potential holding experiment at -0.285 V, appears to produce a more orderly Ag surface. These results confirm recent findings for the same system [16], in which Ag surface rearrangements were promoted by means of combined potential routines. It should be noted that practically no changes can be detected when the potential holding implies either $\theta_{Pb} = 0$ or $\theta_{Pb} \to 1$.

The fact that the greatest efficiency of the potential holding to promote Ag surface rearrangements is found for intermediate values of θ_{Pb} is comparable to that described earlier as the potentiodynamic ageing of O-adatom overlayers on Pt in acid solutions [24]. In this case, the greatest rearrangements of O-adatoms on the Pt surface at the ML level was observed for $\theta_O \cong 0.5$, and the process was related to a place exchange mechanism involving O adatoms and first-layer Pt atoms.

(III.2.2) The influence of Pb upd/stripping for $0 < \theta_{Pb} < 1$

Results comparable to those described previously are obtained when intermediate Pb upd/stripping cycling comprising fractional values of θ_{Pb} is applied, although in this case the potential sweep rate appears as a new variable, as one would expect for a surface rearrangement whose rate apparently depends on θ_{Pb} and $(1 - \theta_{Pb})$, and on the residence time of Pb adatoms on the surface [25].

Fig. 1. Pb upd/stripping voltammograms at 0.01 V/s of Ag overlayers after different electrochemical treatments. 10^{-2} M $Pb(CH_3COO)_2$ + 0.5 M $NaClO_4$ + 10^{-2} M $HClO_4$. The Ag overlayer was prepared in 5×10^{-3} M Ag_2SO_4 + 0.5 M $NaClO_4$ + 10^{-2} M $HClO_4$. $\sigma_d = 156$ mC/cm^2; $\eta = 0.237$ V; 25 °C. (a) Voltammogram after ten cycles; (b) first voltammogram resulting after holding the potential at -0.285 V for 10 min; (c) first voltammogram run immediately after the one shown in (b); (d) 20th voltammogram recorded after the one shown in (b).

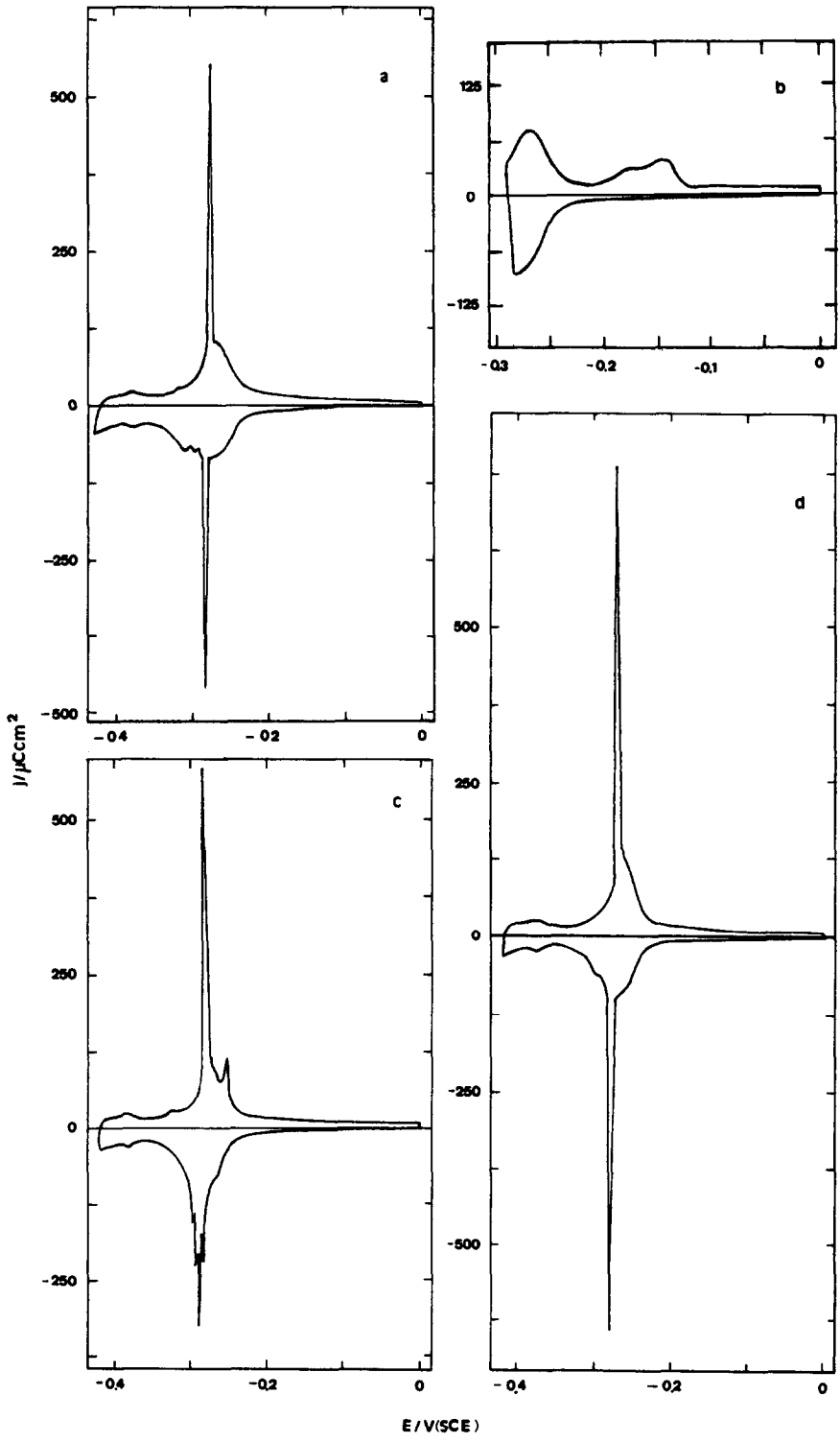
a
b
c
d
500
250
0
-250
-500
125
-125
-0.4
-0.2
0
-0.3
-0.1
j/μCcm²
E/V(SCE)

On the other hand, the Ag surface changes caused by conventional Pb upd/stripping cycling are reflected through a small decrease in the corresponding voltammetric charge, and simultaneously peaks IIa/IIc become sharper than those seen in the initial voltammogram approaching a common height value. These changes are largely comparable to those already described for the voltammogram of upd Pb on Ag (111) for the same conditions [10].

It should be noted that no effect on the voltammetric response of Ag overlayers due to potential cycling in the base electrolyte in the absence of Pb^{2+} ions could be observed.

(III.2.3) Conclusions from the experiments described in Sections (III.2.1) and (III.2.2)

From the preceding experiments the following conclusions can be made:

(i) By holding the potential at a value set within the range where $0 < \theta_{Pb} < 1$, a disordered Ag surface is produced and the probable formation of a Pb + Ag alloy occurs.

(ii) Comparable effects are accomplished by Pb upd/stripping comprising also intermediate θ_{Pb} values.

(iii) The conventional Pb upd/stripping potential range favours the recovery of the initial Ag surface orderly structure. These changes are accompanied by a slight decrease in the voltammetric charge.

(iv) These results are consistent with the mobility of Ag atoms induced by the presence of a fractional Pb adatom monolayer.

(v) Under conventional Pb upd/stripping cycling, the voltammograms after a fixed number of cycles can be used to monitor the characteristics of differently prepared Ag overlayers.

(III.3) The characteristics of Ag overlayers as followed through conventional Pb upd/stripping voltammetry

The influence of the Ag^+ ion concentration in the plating solution, the electrodeposition potential and the electrodeposition charge density on the growth mode of Ag overlayers on polyfaceted Pt single-crystal microspheres were determined by using Pb upd/stripping voltammetry.

(III.3.1) The influence of the Ag_2SO_4 concentration in the plating solution

The conventional Pb upd/stripping voltammogram of Ag overlayers deposited at both constant cathodic overvoltage, $\eta = 0.117$ V ($\eta = E_r - E_d$), and charge density, $\sigma_d = 40$ mC/cm^2, for solution B (Fig. 2a) exhibits a large pair of peaks (IIc–IIa) and another pair of small humps (Ic–Ia and IIIc–IIIa) located on both sides of the pair of peaks IIc–IIa. In addition, a cathodic hump is obtained at ca. -0.33 V as well as an increase in the cathodic current at ca. -0.42 V. The latter should correspond to the initiation of bulk Pb layer growth. The anodic to cathodic charge density ratio derived from the voltammograms is always equal to 1. The voltammogram depicted in Fig. 2a resembles to some extent that described in the literature for Pb upd/strip-

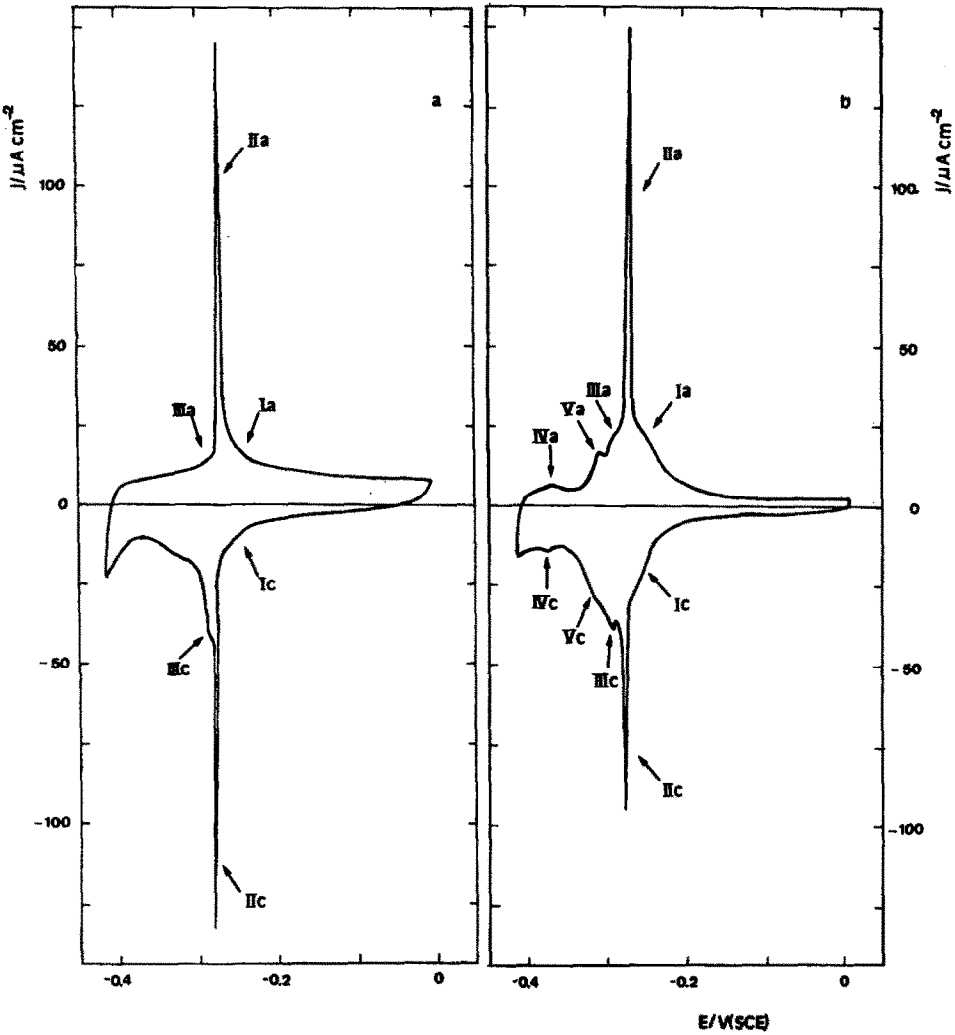

Fig. 2. Influence of the Ag_2SO_4 concentration on the Pb upd/stripping voltammogram (tenth cycle) run at 0.01 V/s. The composition of the solutions was the same as that indicated in Fig. 1 for $\sigma_d = 40$ mC/cm^2 and $\eta = 0.117$ V. (a) $x = 5\times10^{-3}$; (b) $x = 5\times10^{-5}$. 25 °C. The different peaks are identified in the figure.

ping on Ag (111) in similar electrolyte solutions [10–12]. Accordingly, the sharp and large pair of voltammetric peaks IIa–IIc and the two small pairs of peaks IIIa–IIIc and Ia–Ic, on the negative and on the positive potential side of the pair of peaks IIa–IIc, respectively, were assigned to Ag (111) crystal faces.

On the other hand, the voltammograms run on a Ag overlayer grown by decreasing the Ag_2SO_4 concentration (Fig. 2b) exhibit a decrease in the height of the

pair of peaks IIc–IIa and an increase in the contribution of the pairs of peaks Ic–Ia and IIIa–IIIc. Likewise, two new pairs of peaks, IVa–IVc and Va–Vc, at ca. −0.38 and −0.32 V, respectively, and a relative decrease in the cathodic current at −0.42 V, as compared with that shown in Fig. 2a are observed. The potentials of peaks IVc–IVa are close to the potential of the Pb/Pb^{2+} reversible electrode. The voltammogram shown in Fig. 2b presents some features which can be compared with those reported for Pb upd on Ag (100) electrodes in the same solutions [10–12].

Closer inspection of Fig. 2 also reveals that the total voltammetric charge, σ_t, derived from the voltammogram of Fig. 2a ($\sigma_t = 0.600$ mC/cm^2) is about 20% smaller than that resulting from the voltammogram of Fig. 2b ($\sigma_t = 0.780$ mC/cm^2). This charge difference is about the same as that expected for a change from Ag (111) to Ag (100) [10–12].

(III.3.2) The influence of the Ag electrodeposition potential

The influence of E_d on the characteristics of Ag electrodeposits was investigated in 5×10^{-3} M Ag_2SO_4 for a constant σ_d value ($\sigma_d = 40$ mC/cm^2) and values of E_d ranging from 0.437 to 0 V, i.e. in the $0\ V < \eta < 0.437$ V range. Immediately afterwards, the characteristics of the resulting Ag surface were determined through conventional Pb upd/stripping voltammetry (Fig. 3). The following results were obtained from these experiments.

(i) For small values of η, i.e. $\eta < 0.08$ V, the voltammogram (Fig. 3a) shows a small, broad pair of voltammetric peaks, covering nearly the entire potential range of peaks IIa–IIc, Ia–Ic and IIIa–IIIc, as identified in the voltammograms of Fig. 2. The voltammogram depicted in Fig. 3a is similar to that obtained for Pb upd/stripping on a 2 monolayer thick Ag overlayer on the polyfaceted Pt(sc) [22,23], as is described later (Fig. 4).

(ii) For intermediate values of η, i.e. $0.08\ V < \eta < 0.237$ V, the conventional Pb upd/stripping voltammograms resemble greatly that obtained for a Ag (111) electrode under comparable conditions (Fig. 3b).

(iii) For large values of η, i.e. $\eta < 0.237$ V, the shape of the corresponding voltammograms (Fig. 3c) approaches that of a Ag (100) electrode.

(iv) Inspection of the results shown in Fig. 3 also reveals an increase of the Ag surface area by a factor of about 3 as η is increased from 0 to 0.437 V. These experiments suggest that on increasing η, a more open and rough Ag overlayer is obtained, i.e. the Ag growth mode depends considerably on η.

(III.3.3) The influence of the Ag electrodeposition charge density

The value of σ_d was changed from 7.35 to 360 mC/cm^2 for Ag electrodeposits made from 5×10^{-3} M Ag_2SO_4 at $\eta = 0.237$ V. In this case, the conventional Pb upd/stripping voltammograms allow us to derive the following conclusions.

(i) For values of $\sigma_d < 12.4$ mC/cm^2, the voltammogram becomes very close to that already described for a 2 monolayer thick Ag overlayer on Pt substrates (Fig. 4). It should be noted that this comparison can be made only in the potential range between −0.4 and 0 V, because at potentials more positive than 0 V Ag stripping

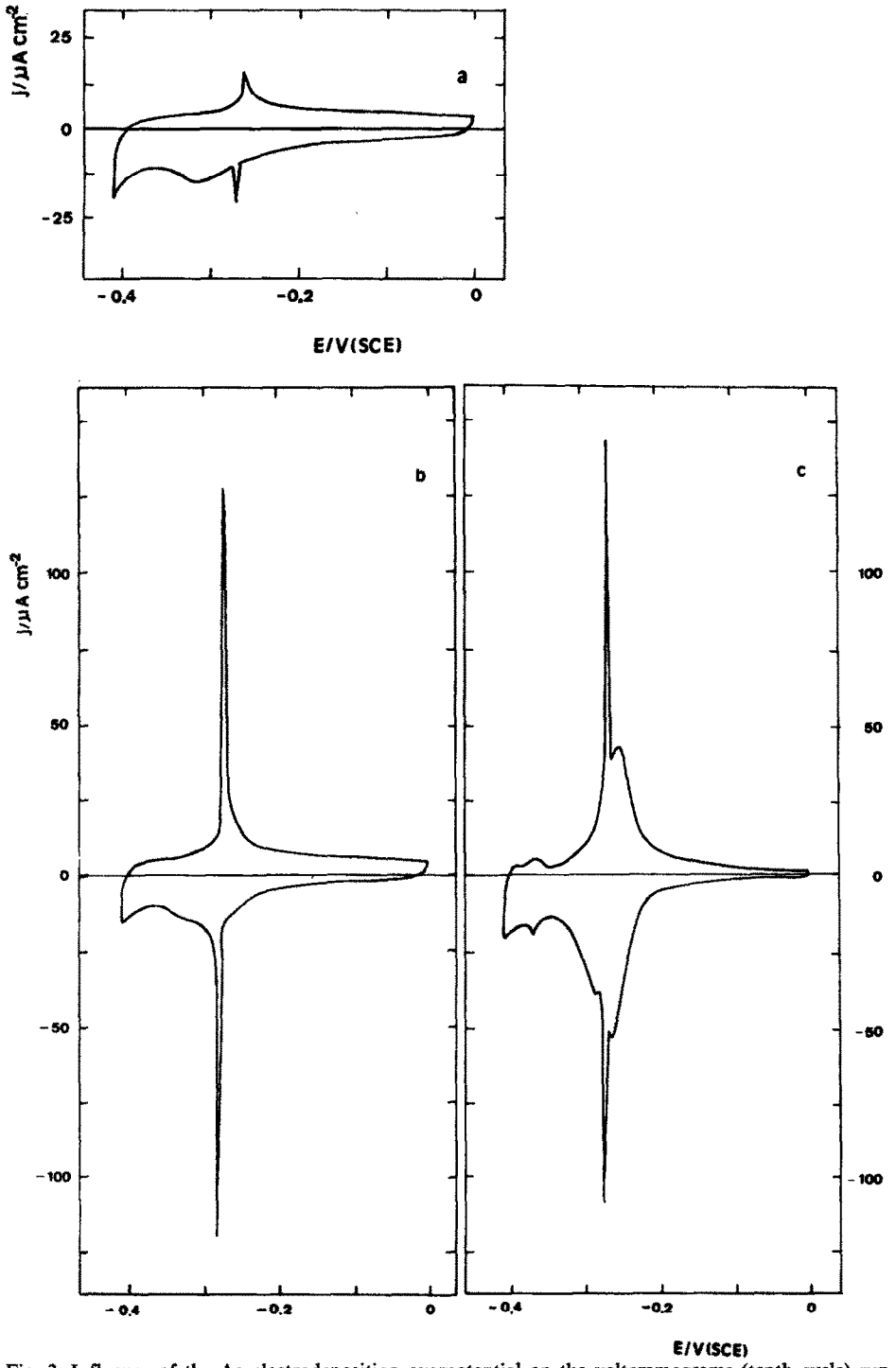

Fig. 3. Influence of the Ag electrodeposition overpotential on the voltammograms (tenth cycle) run at 0.01 V/s for the Pb upd/stripping in the solution indicated in Fig. 2. The electrodeposition of Ag was carried out in 5×10^{-3} M Ag_2SO_4 + 0.5 M $NaClO_4$ + 10^{-2} M $HClO_4$ for $\sigma_d = 40$ mC/cm^2; 25 °C. (a) $\eta = 0.037$ V; (b) $\eta = 0.117$ V; (c) $\eta = 0.437$ V.

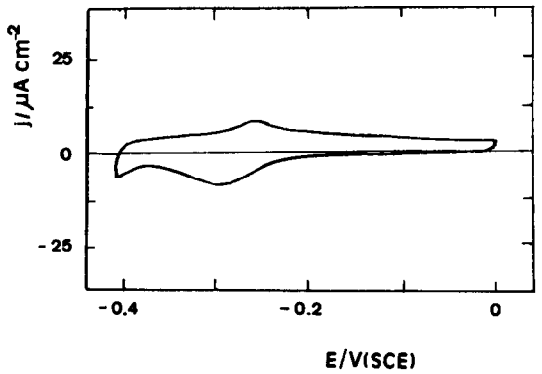

Fig. 4. Voltammogram for Pb upd/stripping (tenth cycle) obtained for a 2 monolayer thickness Ag overlayer on a polyfaceted Pt(sc) electrode run at 0.010 V/s and 25 °C. The composition of the solutions was the same as that in Figs. 2 and 3. η = ca. 0 V.

takes place and the most relevant pair of peaks related to Pb upd/stripping on Pt becomes inaccessible [26,27].

(ii) For $12.4 < \sigma_d < 25.3$ mC/cm^2, well-defined current peaks can be observed. This voltammetric profile points to a preferred crystallographic orientation at the Ag surface leading to Ag (111).

(iii) For $25.3 < \sigma_d < 360$ mC/cm^2, the voltammogram approaches that reported for a Ag (100) electrode under similar operating conditions [10–15].

(iv) A reasonable linear relationship between R, the roughness of the Ag overlayer electrode, and σ_d is obtained (Fig. 5). In this case, the value of R has been

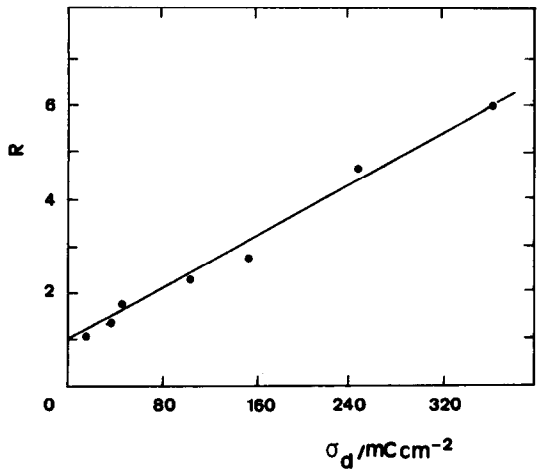

Fig. 5. Plot of roughness factor vs. Ag electrodeposition charge density. The composition of the solutions was the same as that in Figs. 2 and 3; 25 °C. Ag overlayers were prepared at a constant potential, η = 0.237 V.

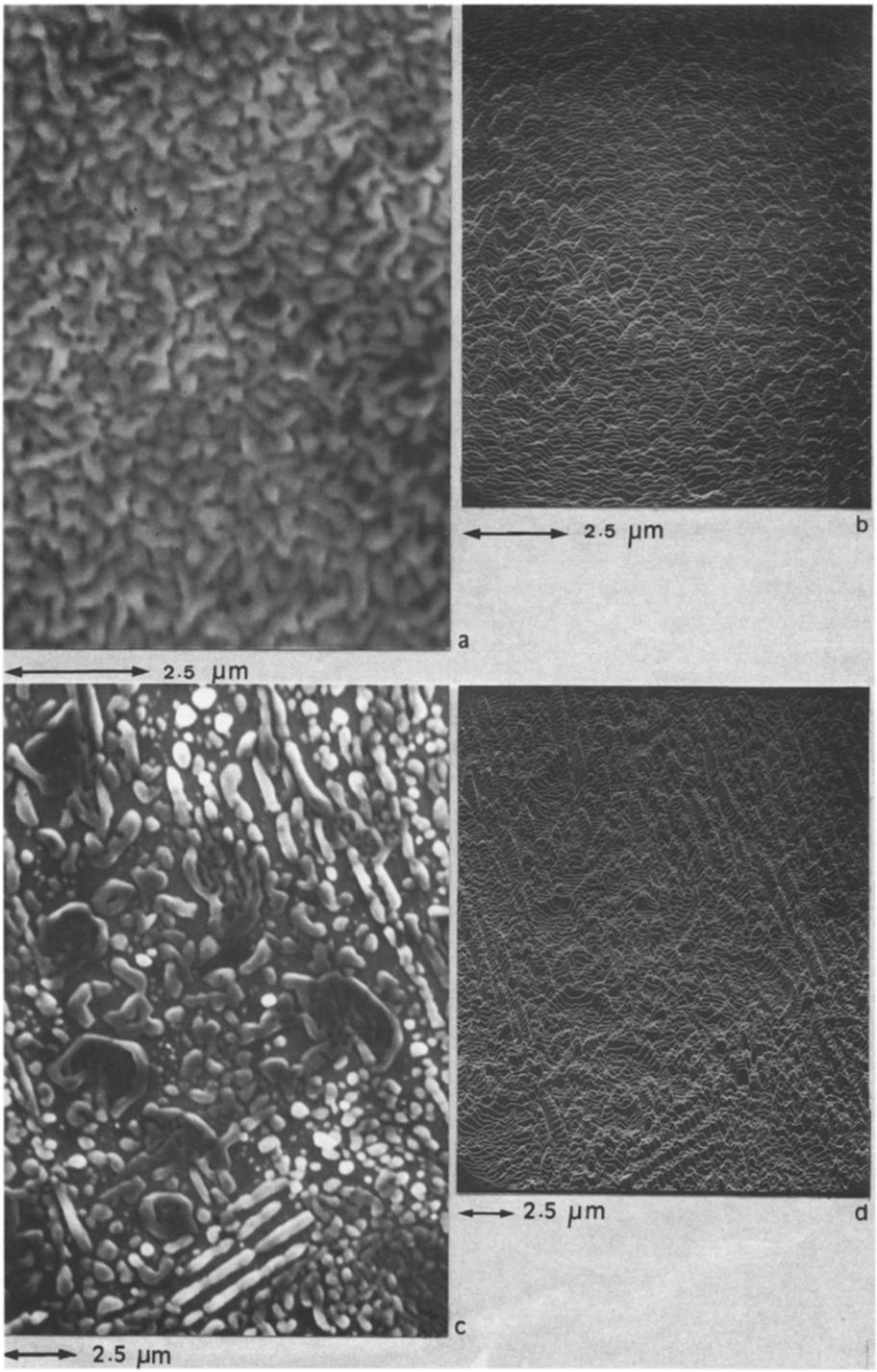

Fig. 6. SEM micrographs. Ag electrodeposits prepared on polyfaceted Pt(sc) by using the solution composition indicated in Fig. 3 for $\sigma_d = 40$ mC/cm^2 and $\eta = 0.117$ V; 25 °C. (a) Ag electrodeposit without Pb upd/stripping cycling; (b) Ag electrodeposit topography; (c) Ag electrodeposit after the Pb /stripping cycling indicated in Figs. 2 and 3; (d) Ag electrodeposit topography.

defined as the quotient between the Pb upd/stripping charge density referred to the geometric electrode area, and the Pb monolayer charge density ($\sigma_{ML} = 0.400$ mC/cm^2) [10–12].

These results show that the behaviour of the Ag electrodeposits at the monolayer level are influenced strongly by the substrate, and the electrochemical behaviour of bulk Ag can be attained only when the number of Ag layers becomes greater than 30.

(III.4) SEM micrographs

SEM micrographs of Ag electrodeposits obtained for $\eta = 0.117$ V and $\sigma_d = 40$ mC/cm^2 reveal the presence of a large number of crystallites covering the entire substrate surface at random (Fig. 6a). The topography of this SEM image is consistent with a rounded top columnar crystallite structure (Fig. 6b). These results are similar to those presented earlier for Au and Pt electrodeposits grown for the electroreduction of the corresponding hydrous metal oxide layers [3,4], except that in the present case the size of the columnar crystallites (average crystallite size in the μm range) is larger than the average size of the crystallites observed for Au and Pt (average crystallite size in the nm range).

The SEM micrograph of a similar Ag electrodeposit resulting after conventional Pb upd/stripping cycling (ten cycles) shows an increase in the crystallite size due to the coalescence of small crystals into larger ones (Fig. 6c). As observed for Au electrodeposits [4], coalescence also results in large voids between the crystals. Besides, the large crystals are oriented in definite directions, as can be seen clearly in the corresponding topographic image (Fig. 6d).

(IV) DISCUSSION

Ag electrodeposition on a polyfaceted Pt(sc) microsphere from acid solutions, as far as the distribution of crystallographic faces and the roughness are concerned, follows similar trends to those already described for other metal electrodeposits such as Au and Pt grown from the electroreduction of the corresponding hydrous metal oxides [3,4,28]. Accordingly, the present results can be discussed by considering firstly those changes which can be reasonably followed through conventional Pb upd/stripping voltammetry, reflecting principally the characteristics of Ag overlayer preparation, and, secondly, those related to the processes mainly responsible for the Ag surface rearrangements.

(IV.1) Growth mode of Ag electrodeposits

(IV.1.1) Crystallographic orientation effects

For a constant Ag electrodeposition charge density exceeding 50 monolayers or thereabouts, the characteristics of Ag deposits change according to the cathodic

overvoltage. Thus, for slowly grown Ag deposits (low η) or deposits grown from a high Ag_2SO_4 concentration in solution, the Ag crystallites exhibit a preferred orientation towards Ag (111), as deduced from conventional Pb upd/stripping voltammograms, i.e. the metal surface structure approaches the most closely packed lattice. This fact agrees with the growth mode of other metal electrodeposits obtained under low cathodic overvoltages from the electroreduction of hydrous metal oxides [4,28,29]. This means that either the slowness of the electrodepositing process provides enough time for the depositing particles to reach the most stable sites or that the number of Ag ions at the interface is sufficiently large to ensure the development of the most compact and stable lattice configuration at the growing overlayer. Conversely, those deposits grown either at high rates (high η) or from dilute Ag_2SO_4 solutions tend to offer an open structure with probably the prevalence of Ag (100). The resulting Ag topography then implies a relative increase in roughness which is most likely due to the appearance of stepped surfaces [11,30]. These surfaces exhibit an inward relaxation which is a function of the surface roughness; the latter is the inverse of the surface packing density [17,18]. In this case, the crystallographic orientation and roughness development effects are intrinsically related, as recently studied for Pt electrodes in acid and alkaline solutions [2,5,31]. The corresponding complex mechanisms of the growth mode were also described through Monte Carlo simulations [32–35].

(IV.1.2) Roughness development. Roughness–melting temperature correlation

The present results allow us to distinguish at least two different types of roughness at the Ag overlayers, namely an atomic roughness which arises from the lack of atomic smoothness which is specific of each crystallographic face of Ag crystallites, and a roughness effect arising from the proper shape factor of Ag crystallites [36]. The atomic roughness may account only for about 20% of the Ag surface area change, but the major change in roughness has to be assigned to the shape factor of Ag crystallites.

The linear dependence of the value of R on σ_d (Fig. 5), which was observed particularly for those Ag electrodeposits grown at high rates (high η), becomes a typical relationship for those systems involving an excess of surface area resulting from columnar microstructures. This is the case, for instance, for Pt and Au deposits grown from the electroreduction of either metal oxides [3,4] or aqueous solutions [37]. The conclusions about the structure of these deposits have been confirmed through STM and combined STM + SEM techniques [29,36,38]. The same behaviour has been found for Rh electrodeposits obtained from the electroreduction of the corresponding hydrous metal oxides [39].

For a rationale of the results shown in Fig. 5, R^*, i.e. the roughness of the deposit expressed per depositing charge unit, was calculated for the four metals indicated in Table 1. It should be noted that the value of R^* decreases in the order Rh > Pt > Au > Ag, and that there is a clear correlation between R^* and T_m, the melting temperature of those metals. The data assembled in Table 1 suggest that the surface diffusion of atoms tends to eliminate the excess of area created during the

TABLE 1

Values of R^* for different metals and melting temperatures

Metal	T_m/°C	(R^*/cm^2 C^{-1}	Reference
Ag	960	16	This work
Au	1063	57	35
Pt	1769	82	33
Rh	1966	590	38

metal overlayer growth under the non-equilibrium conditions determined by the high cathodic overvoltage values.

(IV.1.3) The characteristics of Ag electrodeposits at the monolayer level

The Pb conventional upd/stripping voltammetric behaviour of a 2 monolayer thick Ag overlayer on Pt(sc) microelectrodes (Fig. 4) is comparable to that described for the same reactions on Pt(sc) and definitely distinct from that expected for bulk Ag. This behaviour suggests that at the monolayer level the Ag deposit is influenced considerably by the Pt substrate, the broadness of the voltammetric peaks probably reflecting the polyfaceted characteristics of the Pt electrode. From the present results it appears that the strained layer-by-layer growth for electrodeposits such as Ag on polyfaceted Pt persists at least for a few monolayer thicknesses. However, this effect disappears when the amount of Ag electrodeposited charge is equivalent to about 30 monolayers. These results have a certain parallelism with the growth of evaporated films on different substrates where the growth mode varies according to the orientation and symmetry of the exposed substrate [40–42].

(IV.2) Surface rearrangement processes

The main process associated with the decrease in the Ag surface area can be related to the coalescence of the Ag overlayer structure itself. This conclusion also emerges from observation of the SEM micrographs of Ag deposits before and after the potential cycling treatment in the Pb upd/stripping potential range.

(IV.2.1) A probable mechanism of roughness decay

It is known that roughness decay and surface rearrangements occur spontaneously for metal columnar microstructures in contact with electrolyte solutions [29], although these processes are rather slow for Pt and Au. Otherwise, for these metals the kinetics of roughness decay have been interpreted through a mechanism of coalescence of particles which operates in a tractable way for times of the order of 6×10^4 s and values of R of the order of 60–100.

The present results demonstrate that Ag surface rearrangements for small values of R can be induced in a short time through either potential holding or Pb upd/stripping cycling both involving the $0 < \theta_{Pb} < 1$ range. The former produces an

increase of disorder at the atomic surface lattice, whereas the latter leads to the reverse effect. Otherwise, these processes are accompanied by a change in the value of R for the Ag electrodeposits.

The mechanism of the surface roughness decay and simultaneous change in the crystallographic orientation of the Ag deposited induced through Pb upd/stripping cycling for $0 < \theta_{Pb} < 1$ can be described as follows. The Pb–Ag bond produced through Pb upd should cause distortion over a certain domain of Ag atoms, and in the subsequent stripping process when the Pb–Ag bond is broken, the spacing of Ag atoms participating in Pb–Ag bond formation and rupture should change compared with the initial one. Therefore, one would expect the Ag surface rearrangements to result from the relaxation of those atoms occupying unstable positions in the network.

The same interpretation can be extended to long-range voltammetric cycling even comprising $\theta_{Pb} = 0$ and $\theta_{Pb} = 1$, as for the voltammograms depicted in Fig. 1d run at 0.01 V/s covering a 0.430 V range. In these cases, the average relaxation time for the perturbed Ag atom is about 43 s. On the assumption that the surface diffusion coefficient of Ag atoms is of the order of 1×10^{-12} cm^2/s, the maximum diffusion length for Ag atoms during relaxation is about 80 nm. This is a relatively large diffusion length which enables, after prolonged Pb upd/stripping cycling, rather large crystallites like those seen in the SEM micrographs (Fig. 6) to be obtained. Therefore, the conventional Pb upd/stripping cycling induced rearrangement of the Ag surface results in the ordering of the Ag surface.

According to the preceding surface rearrangement mechanism, Pb upd atoms would cause the expansion of the Ag–Ag interatomic distance at the outer skin region of the Ag overlayer, also allowing to some extent Pb adatoms to penetrate and to produce stronger bonding in the bulk Ag overlayer. This effect is enhanced for the $0 < \theta_{Pb} < 1$ condition at the Ag overlayer surface. The situation is reversed during Pb adatom stripping ($\theta_{Pb} \to 0$), because then the relaxation of the Ag perturbed lattice would go in the direction of producing the closest packing density of Ag atoms. Hence, the degree of order of the Ag surface would depend on how closely and for how long the $\theta_{Pb} \to 0$ condition is approached.

Otherwise, the reaccommodation of the Ag surface induced by the presence of a fractional coverage by Pb adatoms at a constant potential becomes even more complex if penetration of Pb adatoms underneath the first layer of the Ag metal lattice takes place [14]. The latter would become a Ag surface order destructive process, its possible participation depending on the Ag–Ag, Pb–Pb and Ag–Pb bond energies and solubility diagram for the Pb–Ag system. This type of process as well as the experimental conditions for its detection have recently been described for Ag overlayers built up on electrodispersed Pt electrodes in acid solutions [43].

(V) CONCLUSIONS

(1) The growth mode of Ag overlayers on polyfaceted Pt(sc) depends on the cathodic electrodeposition overvoltage and the Ag^+ ion concentration in the solu-

tion. The growth mode involves changes in both the Ag overlayer roughness and the distribution of the crystallographic orientation of crystallites. The increase in the cathodic overvoltage and the decrease in the Ag^+ ion concentration favour the development of roughness.

(2) The present results allow us to establish a correlation between the roughness at metal electrodeposits and the surface diffusion characteristics of metal atoms in contact with the electrolyte solution through the melting temperature of metals.

(3) The Ag overlayers of a few monolayers thickness on the polyfaceted Pt(sc) substrate exhibit a Pb upd/stripping voltammogram which, at least in the potential range where the comparison is feasible, resembles that obtained on the base substrate, as one would expect for a large influence of the substrate on the structure of the thin Ag overlayers.

(4) Rearrangements of the Ag overlayers can be induced by Pb upd/stripping cycling at 0.01 V/s between 0 V ($\theta_{Pb} = 0$) and -0.420 V ($\theta_{Pb} = 1$). These changes appear as a decrease in the roughness of the Ag overlayer and a tendency to produce the most compact packing density of atoms at the metal surface.

(5) The presence of a fractional coverage by Pb adatoms at a constant potential produces changes in the conventional Pb upd/stripping voltammogram which suggest a considerable spontaneous increase of disorder in the structure of the Ag overlayer. This effect can be accomplished by working either potentiostatically or by potential cycling.

ACKNOWLEDGEMENTS

Financial support for this work by the Gobierno de Canarias (Dirección General de Universidades e Investigación) under Research Contract No. 46/01.06.88 is gratefully acknowledged. A.J.A. and R.C.S. thank the Faculty of Chemistry, Universidad de La Laguna for the invitation to cooperate with the Department of Physical Chemistry during 1990.

REFERENCES

1 E.B. Budevski in B.E. Conway, J.O'M Bockris, E. Yeager, S.U.M. Khan and R.E. White (Eds.), Comprehensive Treatise of Electrochemistry, Plenum Press, NY and London, 1983, p. 339.
2 A. Visintin, J.C. Canullo, W.E. Triaca and A.J. Arvia, J. Electroanal. Chem., 239 (1988) 67.
3 A.E. Bolzan, A.M. Castro Luna, A. Visintin, R.C. Salvarezza and A.J. Arvia, Electrochim. Acta, 33 (1988) 1743.
4 A.J. Arvia, R.C. Salvarezza and W.E. Triaca, Electrochim. Acta, 34 (1989) 1057.
5 A. Visintin, J.C. Canullo, W.E. Triaca and A.J. Arvia, J. Electroanal. Chem., 267 (1989) 191.
6 A.C. Chialvo, W.E. Triaca and A.J. Arvia, An. Asoc. Quim. Argent., 73 (1985) 23.
7 T. Kessler, A.M. Castro Luna, W.E. Triaca and A.J. Arvia, J. Appl. Electrochem., 16 (1986) 693.
8 M.L. Marcos, J.M. Vara, J. González Velasco and A.J. Arvia, J. Electroanal. Chem., 224 (1987) 189.
9 A.M. Castro Luna, M.C. Giordano and A.J. Arvia, J. Electroanal. Chem., 259 (1989) 173.
10 A. Bewick and B. Thomas, J. Electroanal. Chem., 84 (1977) 127.
11 H. Bort, K. Juttner, W.J. Lorenz and E. Schmidt, J. Electroanal. Chem., 90 (1978) 413.
12 K. Juttner, Electrochim. Acta, 31 (1986) 917.

13 E. Schmidt and H. Siegenthaler, J. Electroanal. Chem., 150 (1983) 59.
14 A. Popov, N. Dimitrov, O. Velev, T. Vitanov, E. Budevski, E. Schmidt, and H. Siegenthaler, Electrochim. Acta, 34 (1989) 265.
15 A. Hernández Creus, S. González, P. Carro, R.C. Salvarezza and A.J. Arvia, J. Electrochem. Soc., submitted.
16 A.J. Arvia, Surf. Sci., 181 (1987) 78.
17 G.A. Somorjai, Chemistry in Two Dimensions: Surfaces, Cornell University Press, Ithaca, NY, 1981.
18 G.A. Somorjai, J. Phys. Chem., 94 (1990) 1013.
19 F. Jona and P.M. Marcus, The Structure of Surfaces II, Springer Verlag, Berlin and Heidelberg, 1988.
20 J.C. Canullo, W.E. Triaca and A.J. Arvia, J. Electroanal. Chem., 200 (1986) 397.
21 B.E. Conway, H. Angerstein-Kozlowska and W.A. Sharp, Anal. Chem., 45 (1973) 1331.
22 R.C. Salvarezza, D.V. Vásquez Moll, M.C. Giordano and A.J. Arvia, J. Electroanal. Chem., 213 (1986) 301.
23 B. Parajón Costa, J.C. Canullo, R.C. Salvarezza, D.V. Vásquez Moll, M.C. Giordano and A.J. Arvia, J. Electroanal. Chem., 244 (1988) 261.
24 N.E. Folquer, J.O. Zerbino, N.R. de Tacconi and A.J. Arvia, J. Electrochem. Soc., 126 (1979) 592.
25 A. Hernández Creus, P. Carro, S. González, R.C. Salvarezza and A.J. Arvia, J. Electroanal. Chem., to be submitted.
26 D.M. Kolb, R. Kotzan and D.L. Rath, Surf. Sci., 101 (1980) 490.
27 F. El Omar and R. Durand, J. Electroanal. Chem., 178 (1984) 343.
28 C. Alonso, R.C. Salvarezza, J.M. Vara and A.J. Arvia, Electrochim. Acta, in press.
29 C. Alonso, R.C. Salvarezza, J.M. Vara, A.J. Arvia, L. Vázquez, A. Bartolomé and A.M. Baró, J. Electrochem. Soc., 137 (1990) 2161.
30 J.C. Canullo, H.L. Tignanelli, A. Plastino and A.J. Arvia, Langmuir, in press.
31 A. Visintin, W.E. Triaca and A.J. Arvia, J. Electroanal. Chem., 284 (1990) 465.
32 E.V. Albano, H.O. Martin and A.J. Arvia, Electrochim. Acta, 33 (1988) 271.
33 E.V. Albano, H.O. Martin, R.C. Salvarezza, M.E. Vela and A.J. Arvia, J. Electrochem. Soc., 137 (1990) 117.
34 R.C. Salvarezza, J.M. Vara, E.V. Albano, H.O. Martin and A.J. Arvia, Phys. Rev., 41 (1990) 12495.
35 R.C. Salvarezza, C. Alonso, J.M. Vara, E.V. Albano, H.O. Martin and A.J. Arvia, Phys. Rev., submitted.
36 L. Vázquez, A. Bartolomé, A.M. Baró, C. Alonso, R.C. Salvarezza and A.J. Arvia, Surv. Sci., 215 (1989) 171.
37 K. Shimazu, K. Uosaki and H. Kita, J. Electroanal. Chem., 256 (1988) 481.
38 R.C. Salvarezza, J.M. Vara and A.J. Arvia, in preparation.
39 A.C. Chialvo, W.E. Triaca and A.J. Arvia, J. Electroanal. Chem., 237 (1987) 237.
40 C. Binns, C. Norris, G.C. Smith, H.A. Padmore and M.G. Barthes-Labrousse, Surf. Sci., 126 (1983) 158.
41 F. El-Omar, R. Durand and R. Faure, J. Electroanal. Chem., 160 (1984) 385.
42 A. Clark, P.J. Rous, J. Arnott, G. Jennings and R.F. Willis, Surf. Sci., 192 (1987) L43.
43 M.E. Martins, R.C. Salvarezza and A.J. Arvia, Electrochim. Acta, in press.